Remote Sensing of Environment 124 (2012) 38–48

Contents lists available at SciVerse ScienceDirect

Remote Sensing of Environment

journal homepage: www.elsevier.com/locate/rse

Phytoplankton bloom during the northeast monsoon in the Luzon Strait bordering the Kuroshio

Shaoling Shang [a,b,*], Li Li [c], Jun Li [a], Yonghong Li [a], Gong Lin [a], Jun Sun [d]

[a] State Key Laboratory of Marine Environmental Science, Xiamen University, Xiamen 361005, China
[b] Research and Development Center for Ocean Observation Technologies, Xiamen University, Xiamen 361005, China
[c] The Third Institute of Oceanography, State Oceanic Administration, Xiamen 361005, China
[d] College of Marine Science and Engineering, Tianjin University of Science and Technology, Tianjin 300457, China

ARTICLE INFO

Article history:
Received 10 November 2011
Received in revised form 27 March 2012
Accepted 22 April 2012
Available online xxxx

Keywords:
Bloom
Phytoplankton absorption coefficient
Remote sensing
Kuroshio intrusion
Luzon Strait
South China Sea

ABSTRACT

Several studies have reported intensive phytoplankton blooms during the northeast monsoon season in the Luzon Strait and its vicinity (the "LZS bloom"); the primary mechanism underlying this phenomenon is however not yet clear. Here we investigated the January 2010 LZS bloom and climatological state using *in situ* and remote sensing data, including the MODIS phytoplankton absorption coefficient at 443 nm (Aph) as a preferable pigmentation index. Blooming patches of Aph $\geq 0.02\ m^{-1}$ overlaid on a background level of $0.01\ m^{-1}$ were discernible for both situations. A twin-core structure of the bloom was identified; the major core lay far offshore in the deep basin to the northwest of Luzon, with a maximum horizontal scale of ~250 km, and the other core was nearshore in the Babuyan Channel, with a maximum scale of ~100 km. Variations in climatological monthly mean Aph indicate that the LZS bloom as a whole persists from November to February, peaking in December. Further investigations with satellite altimetry and sea surface temperature suggest that the bloom is primarily associated with the Kuroshio and its intrusion, which generate various meso-scale processes and thus induce enhanced nutrient pumping/entrainment from depth when interacting with the topography of the Luzon Strait and the circulation of the northeastern South China Sea (i.e. the Luzon Gyre). Meanwhile, upwelling at the center of the Luzon Gyre contributes to the offshore bloom. The nearshore bloom is substantially enhanced by nutrient input from the Cagayan River.

1. Introduction

The Luzon Strait (LZS) is the major channel allowing exchange of water between the South China Sea (SCS) and the western Pacific. During the northeast monsoon season, the Kuroshio invades the SCS through the LZS (Li et al., 2000; Shaw & Chao, 1994; Wyrtki, 1961), while phytoplankton blooms form frequently to the west of the LZS (Chen et al., 2006, 2007; Liu et al., 2002; O'Reilly et al., 2000; Penaflor et al., 2007; Tang et al., 1999). Most studies of these blooms were based on chlorophyll-*a* concentration (Chl) derived empirically from satellite (CZCS, SeaWiFS, and MODIS) observations (Fig. 1). *In situ* observations were also reported for limited stations between 18–19°N, 118.0–118.5°E and at ~20°N, 120°E (Chen et al., 2006, 2007; Liu et al., 2002; Fig. 1). We here refer phytoplankton blooms in this region as the LZS bloom.

Most previous studies (Chen et al., 2006; Liu et al., 2002; Tang et al., 1999) attributed recurrence of the LZS bloom to a localized upwelling off northwest Luzon, which is present from below the mixed layer to ~300 m and is centered ~100 km off northwest Luzon between 16°N and 19°N (Shaw et al., 1996; Udarbe-Walker & Villanoy, 2001). Wang et al. (2010) emphasized the role of wind-driven mixed layer entrainment, since the surface bloom cannot be fully explained by subsurface upwelling, while Penaflor et al. (2007) suggested that the bloom intensity was likely influenced by current interaction of the upwelling induced by uplift of the northward-flowing Luzon Coastal Current as it encounters the Kuroshio intrusion. Chen et al. (2007) provided the first report that enhanced productivity in the LZS in April 2005 was associated with a cold-core eddy, which was thought to be shed from the Kuroshio intrusion. These reports indicate that the origin of the LZS bloom remains under debate.

In addition, most previous satellite images of Chl show that, concurrent with the offshore bloom to the west of the LZS, Chl levels also appear high in the southern LZS, especially along the northern coast of Luzon. This phenomenon has been neglected by most studies, with the exception of one report (Penaflor et al., 2007) suggesting the potential influence of river inputs in the vicinity of the northern Luzon coast, where Chl levels are constantly high throughout the year. Chl products derived with band-ratio empirical algorithms usually suffer from interference from other optically active components

* Corresponding author at: State Key Laboratory of Marine Environmental Science, Xiamen University, Xiamen 361005, China. Tel.: +86 592 2184781; fax: +86 592 2184781.
E-mail addresses: slshang@gmail.com, slshang@xmu.edu.cn (S. Shang).

0034-4257/$ – see front matter © 2012 Elsevier Inc. All rights reserved.
doi:10.1016/j.rse.2012.04.022

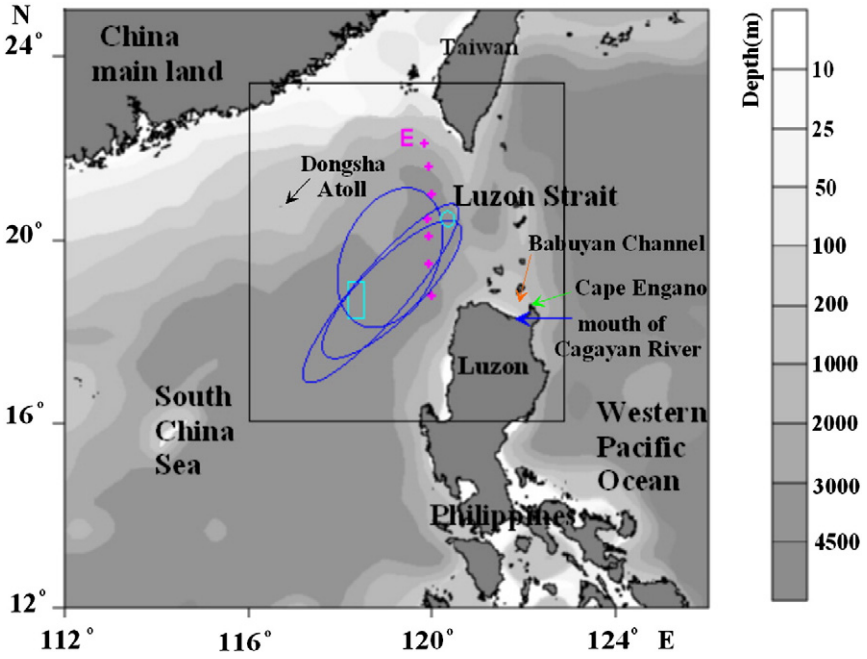

Fig. 1. Map of the South China Sea with bathymetry; the black box shows the study region-the northeastern South China Sea including the Luzon Strait, for which remote sensing data were processed (16 -23°N, 116–123°E); E refer to one transect surveyed during January 27–30, 2010; seven stations of E transect are numbered as E400-E406 from north to south (the purple crosses); the cyan box and circle show the previous reported blooming area based on *in situ* observations (Chen et al., 2006, 2007; Liu et al., 2002); the blue ellipses roughly represent the previous reported blooming areas based on satellite observations (Liu et al., 2002; Penaflor et al., 2007; Wang et al., 2010).

(color dissolved organic matters and particulate detritus) in the near-shore water, and thus it remains unknown whether the high Chl levels in the southern LZS derived from satellite measurements are part of the LZS bloom.

Here we investigate the LZS bloom via *in situ* and remote sensing observations, using the analytically derived phytoplankton absorption coefficient at 443 nm (Aph) to characterize the bloom in order to discriminate real phytoplankton signals from other color-active components. The use of phytoplankton absorption as a superior metric of phytoplankton pigmentation, instead of band-ratio derived Chl levels, is increasingly accepted as a valid method (e.g. Cullen, 1982; Marra et al., 2007), especially from the remote-sensing point of view (Hirawake et al., 2011; Lee et al., 1996, 2011). A MODIS Aph time-series study has demonstrated that Aph can serve as the preferred index for characterizing phytoplankton variability in the upper ocean (Shang et al., 2011). Nevertheless, we also include fluorescence line height (FLH) and conventional empirically derived Chl data for further justification of Aph in interpreting phytoplankton dynamics. FLH was developed to estimate sun-stimulated chlorophyll fluorescence (Gower, 1980), which is also less sensitive to interference caused by non-biotic optically active materials (Letelier & Abbott, 1996); this property is thus suitable for intense coastal bloom detection (e.g. Hu et al., 2004). Finally, we evaluate remote sensing altimetry and sea surface temperature (SST), as well as *in situ* salinity, temperature, and Aph measurements to aid in our interpretation of the LZS bloom. Overall, we wish to address where and when the LZS bloom initiates and progresses, and what triggers and sustains the LZS bloom. These results will provide a more comprehensive insight of the biogeochemistry for waters around the Luzon Strait.

2. Data and methods

2.1. Study region

The northeastern SCS, including the LZS, is the region under study (Fig. 1). The LZS, with a sill depth of ~2400 m, is between the southern tip of Taiwan and the northern coast of Luzon. There are several islands located at the southern LZS. Between the islands and the northern coast of Luzon is the relatively shallow (~200 m depth) Babuyan Channel, where the LZS receives the Cagayan River, the longest river in the Philippines. We processed remote sensing data from 16 to 23°N, 116 to 123°E (see the black square in Fig. 1). Calculation of the spatial mean and other statistics was restricted to the east of the Dongsha Atoll and to the south of Taiwan in order to discriminate the LZS bloom from the productive coastal waters offshore Taiwan and mainland China.

2.2. Remote sensing data

Aqua-MODIS daily Level-3 remote sensing reflectance (R_{rs}, sr^{-1}; Version r2009.1), FLH, and Chl data of January 28, 2010, when *in situ* measurements were available, were downloaded from the NASA Distributed Active Archive Center (DAAC, http://oceancolor.gsfc.nasa.gov/). The spatial resolution of these data was 1 km by 1 km. The R_{rs} data were then fed to a quasi-analytical algorithm (QAA) to derive Aph. Detailed description and steps can be found in Lee et al. (2002, 2007, 2010). Computer codes for the derivation can be found at the IOCCG website (http://www.ioccg.org/groups/software.html). Briefly, coefficients of total absorption and backscattering of the water are derived from R_{rs} based on a radiative transfer model. Then spectral models for the absorption coefficient of phytoplankton pigments, color dissolved organic matters and particulate detritus are involved to analytically decompose the total absorption coefficients into phytoplankton absorption coefficients and the non-pigment absorption coefficients at multiple bands. Among all the derived products, only Aph, which primarily represents the absorption coefficient of chlorophyll-*a* (has an absorption peak at ~443 nm), was used in this study. MODIS FLH is a standard product released by NASA and is derived from three MODIS Bands centered at 665, 678, and 746 nm (Letelier & Abbott, 1996). Chl were derived using the OC3M empirical band-ratio algorithm (O'Reilly et al., 2000). In order to acquire a climatology of Aph in the study region, Aqua-MODIS monthly Level-3 R_{rs} data from January 2003 to December 2010 were obtained from the NASA DAAC. The spatial resolution of these data was 4 km by 4 km, and the R_{rs} data were fed to the QAA to

derive monthly mean Aph for 2003–2010, which were then averaged to produce climatological monthly means. The Terra-MODIS daily Level-3 SST on January 28, 2010 and the climatological monthly mean SST from July 2002–February 2011 (Aqua-MODIS) were also retrieved from the NASA DAAC.

Altimetry products used in this study included a 7 day gridded Absolute Dynamic Topography (ADT) product for January 27, 2010 to February 3, 2010 , the climatological monthly mean sea level anomaly data (1993–2010), and the climatological monthly mean dynamic topography data (1993–2010, entitled MDT_CNES-CLS09). The former two were produced by Ssalto/*Duacs* and distributed by *Aviso* with support from *Cnes* (http://www.aviso.oceanobs.com), while MDT_CNES-CLS09 was produced by *CLS* Space Oceanography Division and also distributed by *Aviso*. The climatological monthly mean ADT in December was then computed by adding the climatological monthly mean sea level anomaly in December to MDT_CNES-CLS09 in the same month.

2.3. In situ observations

In situ measurements of absorption coefficients, temperature, and salinity in the study region were carried out in January 2010 (Fig. 1). The particulate absorption coefficient (m^{-1}) was measured by the filter-pad technique (Kiefer & SooHoo, 1982) with a dual-beam PE Lambda 950 spectrophotometer equipped with an integrating sphere (150 mm in diameter) following a modified transmittance-reflectance method (Dong et al., 2008; Tassan & Ferrari, 2002). Detrital absorption (m^{-1}) was obtained by repeating the modified transmittance–reflectance measurements on samples after pigment extraction with methanol (Kishino et al., 1985). Phytoplankton absorption coefficient was then calculated by subtracting the detrital absorption from the particulate absorption coefficient. Salinity and temperature was recorded with a Seabird CTD (SBE 19).

Climatological monthly means of temperature in the study region in December were obtained from the National Oceanographic Data Center (Locarnini et al., 2006). Cagayan River discharge data was downloaded from the SAGE River Discharge Database at http://www.sage.wisc.edu/riverdata/.

3. The LZS bloom observed in January 2010

Field Aph data measured along ~119.6°E (Fig. 1) during January 27–30, 2010 clearly revealed a high production patch in the middle of the surveyed transect (Fig. 2a). Note that in general the background Aph in the SCS basin is ~0.01 m^{-1} (Shang, unpublished data). For the transect under survey, in general the Aph remained >0.02 m^{-1} through the upper 50 m and decreased monotonically downward, except at Station E406, the southernmost station. These measurements indicate that a bloom occurred in this water. Horizontally, Aph was especially high in the upper layer from Stations E403-405 ranging from 0.034 to 0.054 m^{-1}. Nevertheless, vertical distribution of Aph differed between stations. A distinct subsurface maximum at ~50 m was found at Station E406, the only site where surface Aph was less than 0.02 m^{-1}. Weaker subsurface maximums were also observed at ~25 m at Stations E404 and 405. In contrast, Aph decreased sharply at Station E403 from a surface value of 0.054 m^{-1}, the highest Aph observed during the survey, to a background level at ~75 m.

A similar pattern of horizontal and vertical distribution of Chl concentration was detected in field measurements (Fig. 2a). The upper-layer Chl concentration was >0.6 mg/m^3 at Stations E403–405, while it was ~0.4–0.5 mg/m^3 to the north and <0.3 mg/m^3 to the south. Chen et al. (2006) observed similarly high surface Chl concentrations (0.4–0.6 mg/m^3) in January 1999 at 19°N, 118.5°E, approximately one degree west of our E transect. Chen et al. (2007) also reported surface Chl concentrations up to 0.4 mg/m^3 in April 2005 at ~20°15'N, 120°31'E, a site close to Station E404 in this study.

A MODIS Aph image acquired on January 28, 2010 supported the strikingly broad coverage and substantial intensity of the bloom as revealed by our *in situ* observations (Fig. 2b). A large patch of Aph ≥0.02 m^{-1} occurred in the middle of the study region, overlaid on a background of ~0.01 m^{-1}. The patch extended from the southern LZS to the Dongsha Atoll, forming an upside-down "V" with the E transect across its west wing. The patch consisted of two major portions, a large offshore subpatch to the west of the LZS centered at ~19.5°N, 119.5°E with a horizontal scale of ~250 km, and a smaller portion in the southern LZS near the Luzon coast centered at ~19°N, 121.5°E with a scale of ~100 km. In both portions, the Aph maximum was >0.1 m^{-1}.

The concurrent MODIS FLH snapshot indicated a consistent blooming patch (Fig. 2c). An upside-down "V" of FLH ≥0.010 mW cm^{-2} μm^{-1} sr^{-1} overlaid on a background of ~0.005 mW cm^{-2} μm^{-1} sr^{-1} was consistent with the Aph measurements. This also implicates that for those ocean color sensors without the capability of FLH measurement, such as SeaWiFS and VIIRS, analytically derived Aph can be valuable for bloom detection and interpretation, either in nearshore or offshore waters. Meanwhile, the conventional, empirically derived Chl concentration, which is in principle a convincing metric for bloom detection for waters with constituents dominated by phytoplankton, also revealed a bloom patch of the same size and shape (Fig. 2d).

In summary, in agreement with previous reports, an intense phytoplankton bloom occurred in the deep winter of January 2010 in the LZS, extending to the northeastern SCS and covering the area of ~17–22°N, ~117–122°E. The maximum Aph and Chl measurements observed *in situ* at six sampling stations were 0.05 m^{-1} and 0.8 mg/m^3, respectively, while the maximum Aph acquired from MODIS was >0.1 m^{-1} (not captured *in situ* due to sparse spatial resolution). Taken together, these observations affirmed the LZS bloom as a phenomenon that emerged in the northeast monsoon season and suggested that the fine structure of the bloom deserves further exploration.

4. Climatological variations in the LZS bloom

In order to better characterize the LZS bloom, climatological monthly mean MODIS Aph data (Fig. 3) were evaluated for the region 16–23°N, 116–123°E. The spatial Aph mean was also derived from this dataset to quantitatively illustrate the annual variation in bloom intensity. It was calculated for 17.5–21.5°N, 117.5–122.4°E (see the large white rectangle in Fig. 3 in image of December) and shown in Fig. 4.

From April to September, Aph in the study region remained low, with the exception of the nearshore water of northern Luzon (Fig. 3). Mean Aph remained at the background level of ~0.010 m^{-1} (Fig. 4). A rise in Aph began in October, when small patches of Aph ≥0.02 m^{-1} emerged offshore (Fig. 3). Mean Aph jumped abruptly in November, reflecting initiation of an intense bloom. At this time, however, the offshore blooming patch was still restricted to the mid-LZS, while the nearshore blooming patch covered the entire Babuyan Channel. In December, the high Aph patch enlarged substantially to encompass the region west to the LZS as far as the Dongsha Atoll. It manifested itself like the bloom event observed on January 28, 2010 (Fig. 2), registering an offshore core of Aph ≥0.03 m^{-1} in the area of ~19–20.5°N, 119.5–121°E and a core near the northern Luzon coast. In January, the patch maintained its shape but weakened, as indicated by the mean Aph values (Fig. 4). Decline of the bloom continued in February, when the blooming patch retreated to the nearshore area of northern Luzon. The mean Aph values finally dropped to background levels in March (Fig. 4), although a small patch of Aph ≥0.02 m^{-1} remained in the southern LZS (Fig. 3).

Two separate cores of the LZS bloom, one offshore and another nearshore, were also prominent (Fig. 3), as observed in January 2010 (Fig. 2b). The nearshore subpatch in the southern LZS, although small in size, appeared to progress differently from the offshore

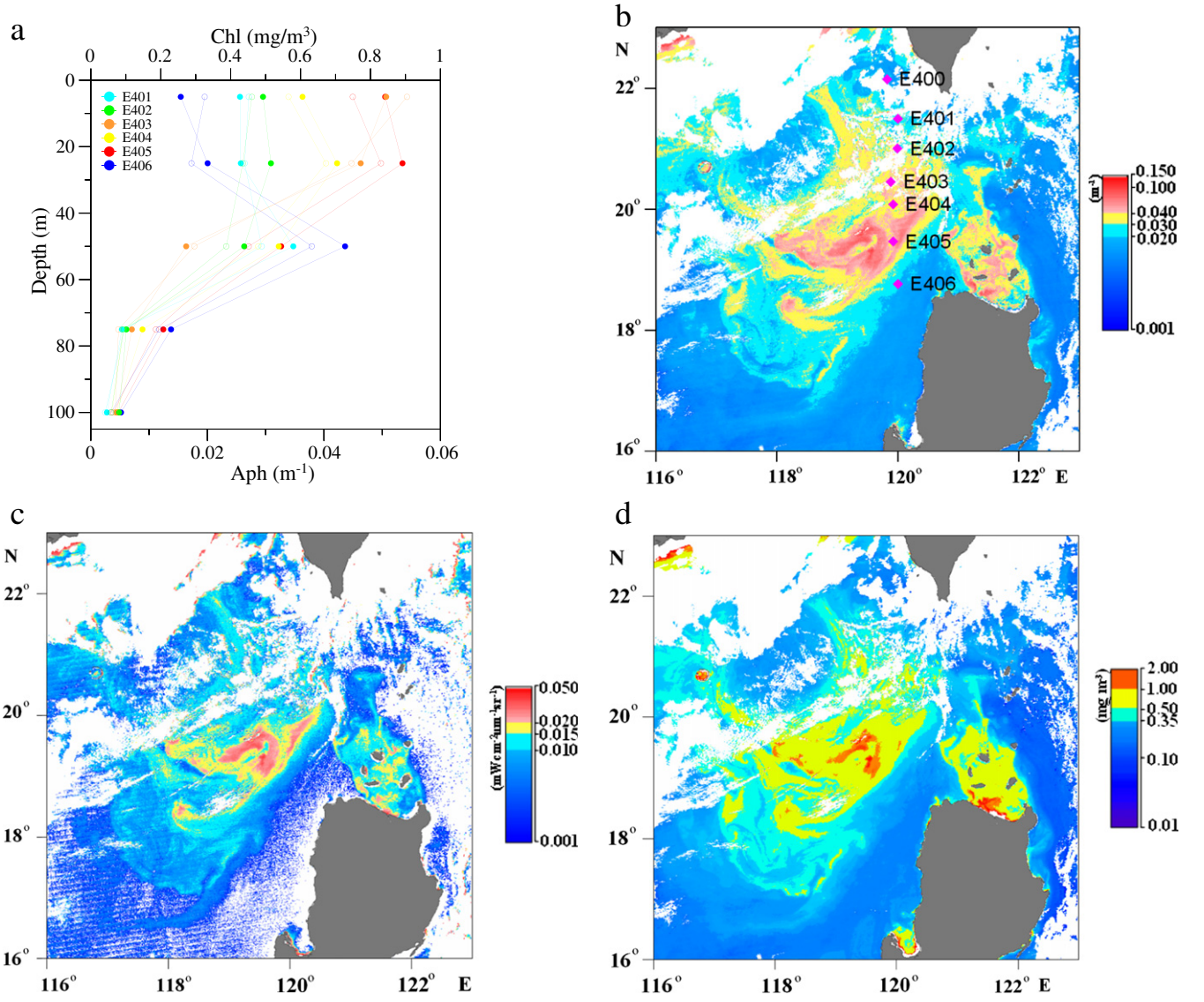

Fig. 2. *In situ* Aph (empty circles) and Chl (solid circles) observed during January 27–30, 2010; note that Aph and Chl at station E400 was missing (a); MODIS Aph (b), FLH (c) and Chl (d) on January 28, 2010; purple diamonds on the Aph image indicate the location of Stations E400-E406.

portion. A close-up view of Aph in the southern LZS (18-20°N, 120–122.4°E) revealed several notable temporal-spatial features of its seasonal evolution (Fig. 5). Aph was $>0.02\ m^{-1}$ most of the time (except spring) in the very immediate vicinity of the mouth of the Cagayan River. Seasonal expansion of the high Aph area occurred down the coast away from the river mouth and was associated with an Aph increase in fall and decay in late winter. A patch of Aph $\geq 0.04\ m^{-1}$ appeared in November and December.

To clarify and quantify the nearshore portion of the LZS bloom, we specifically derived the annual variation in spatial mean Aph within the Babuyan Channel (see the white rectangle in Fig. 5 the December image), where the core of the nearshore bloom is located. The spatial mean Aph measurement remained low in spring and summer, exceeded $0.02\ m^{-1}$ in October, and achieved its maximum value of $0.032\ m^{-1}$ in December (Fig. 4). This confirmed that the nearshore bloom was triggered in October and persisted until February the following year. Its triggering time was one month earlier than that of the major, offshore portion of the LZS bloom. Interestingly, the nearshore and offshore blooms consistently peaked in December and ceased in March. These temporal discrepancy/consistency suggested differences in bloom driving mechanisms in the nearshore and the offshore waters (see Section 5).

Therefore, both field observations and climatological analyses revealed a unique twin-core structure of the LZS bloom during the northeast monsoon season. The major core lay far offshore in the deep basin to the northwest of Luzon (centered at ~19.6°N, 120°E), while the other core was nearshore in the Babuyan Channel. The offshore core of the LZS bloom and its distribution observed in this study are similar to reports based on satellite Chl from various sensors in different years (Liu et al., 2002; Penaflor et al., 2007). The results presented here, on the other hand, for the first time document the existence of a nearshore core, which was not previously recognized as part of the LZS bloom due to the caution commonly employed when using empirically-derived Chl in the vicinity of the Babuyan Channel, an area of optical complexity owing to river inputs.

5. Discussion

Based on MODIS Aph, FLH, and Chl data and *in situ* biological properties, we confirmed a strong bloom extending from the southern LZS

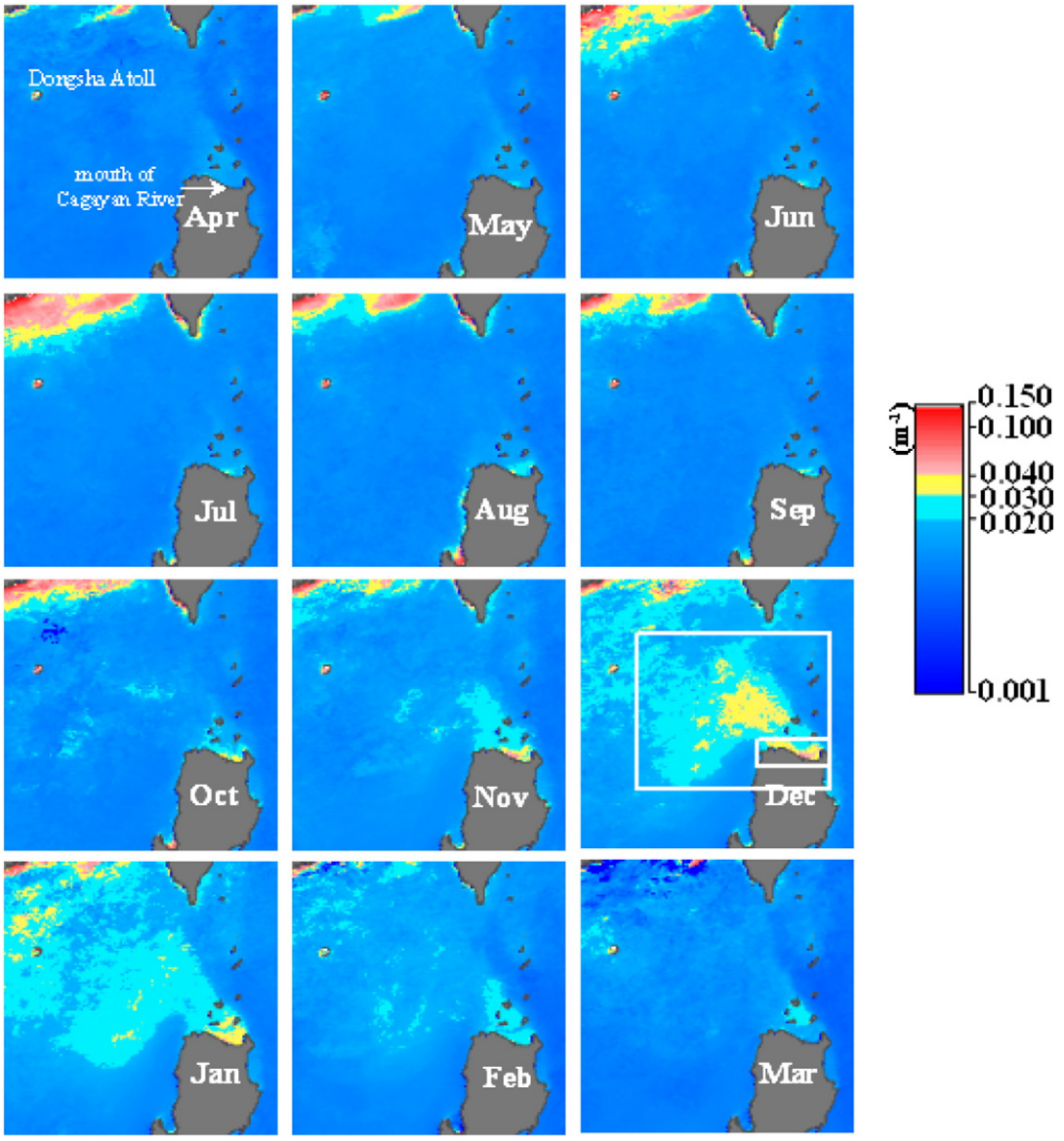

Fig. 3. Climatological monthly mean MODIS Aph in the Luzon Strait and its vicinity.

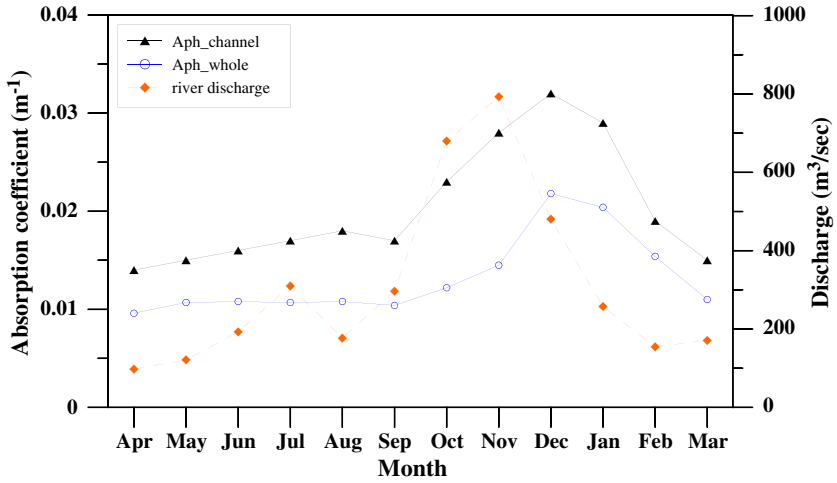

Fig. 4. Variations of climatological monthly mean MODIS Aph averaged for the area of 17.5–21.5°N, 117.5–122.4°E (labeled as Aph_whole; see the large white box in Fig. 3 December image for the area) and averaged for the Babuyan Channel (labeled as Aph_channel; see the small white box in Figs. 3 and 5 December image for the area), and the climatological monthly mean discharge of the Cagayan River.

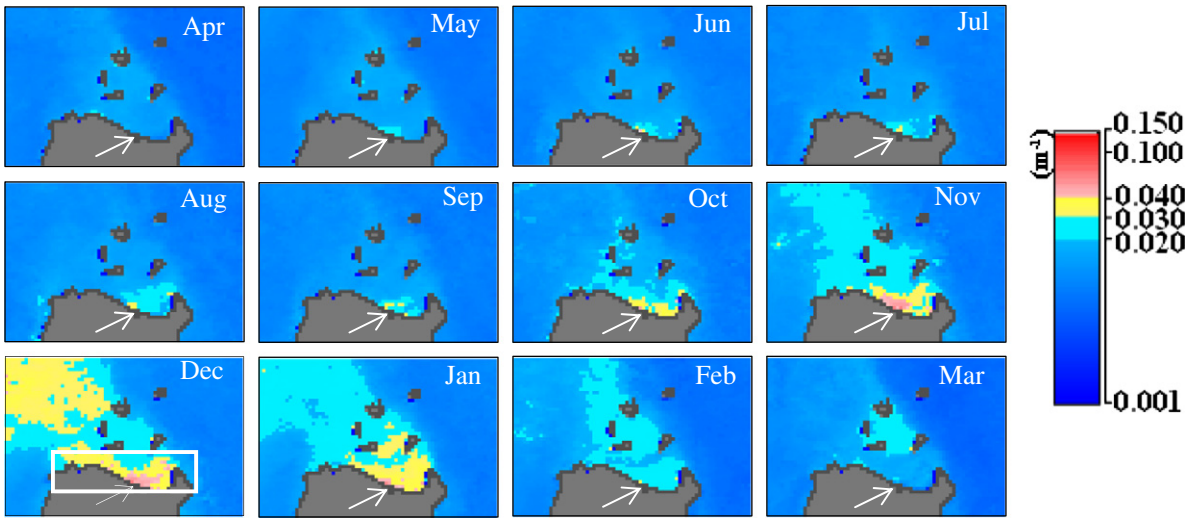

Fig. 5. A close-up view of MODIS Aph for the southern Luzon Strait (18–20°N, 120–123°E); the white arrow points to the location of the Cagayan River mouth.

to the east of the Dongsha Atoll in January 2010. Climatologically, this bloom emerges steadily from November to February. We also found, for the first time, that a small portion of the bloom was located nearshore in the Babuyan Channel and its vicinity, and was strong and persistent for five months (October–February, one month earlier than the triggering time of the large offshore portion). Following we discuss the mechanisms underlying these spatio-temporal characteristics of the LZS bloom.

5.1. Environment of the LZS bloom

In order to tackle the driving mechanisms for the LZS bloom, the environmental processes, through which nutrients can be brought into the euphotic zone for phytoplankton to thrive, deserve exploration, since nitrate availability has been found to be a critical factor in the growth of phytoplankton in the SCS (Chen, 2005).

5.1.1. The January 2010 case

Fig. 6a shows that, in January 2010, surface circulation of the study area was dominated by the Kuroshio (labeled as K on Fig. 6a) and the Luzon Gyre (LG; Fang et al., 1998; Wang et al., 2008), as indicated by the strong bend of the satellite altimetry ADT high to the SCS through the northern LZS, and the presence of large ADT low bordering the Kuroshio. MODIS SST was obviously low at the center of the LG, indicating upwelling at the center of the LG that brings cold water from depth towards the surface. An isolated ADT high (labeled as H on Fig. 6a) centered at ~20.5°N, 118°E to the west of the LG was also detected, suggesting an anticyclonic eddy likely shed from the Kuroshio (Li et al., 1998) or as a form of Kuroshio penetration (Hu et al., 2012). This Kuroshio associated anticyclonic eddy, however, exhibited no corresponding surface warm pool on the MODIS SST image, probably because the surface was covered by cold water spread from the mainland China coast. The SST image also reveals that the Luzon Coastal Current, which flows along the west coast of Luzon, carries warm water from the SCS basin to the northern SCS. The Aph image (Fig. 6b) in combination with the SST image (Fig. 6a) further show that the offshore Aph high lay mainly on the northern sector of the LG, with its core matching with the LG center, and with the Kuroshio to the east and the detached anticyclonic eddy to the west. In contrast, the ADT high to the west of the LG was accompanied by a pool of low Aph.

The *in situ* observations on temperature and salinity along the E transect (see diamonds on Fig. 6b for location of sampling stations) were consistent with the MODIS observations of LG upwelling. Domed isolines at Station E404 nearby the LG center were visible in Fig. 6c. Domed isotherm also occurred at Station E401, indicating a front associated with the intrusion of Kuroshio into the Taiwan Strait.

Zooming in the southern LZS, where the nearshore portion of the LZS bloom occurred, we found a small-scale ADT low (labeled as L on Fig. 6a) behind Cape Engano (labeled as CE on Fig. 6a). Corresponding MODIS SST low was discernible, suggesting upwelling that brings cold water from depth towards the surface (Fig. 6a). Nevertheless, the cold water was not restricted to the area behind the cape. It also covered the surrounding islands. Such an ADT low and associated cold water mass could be attributed to lee eddies and turbulent mixing frequently observed when a strong current passes by oceanic barriers (e.g. Aristegui et al., 1997; Signorini et al., 1999). Besides, the Cagayan River (labeled as CR on Fig. 6a) discharges into the Babuyan Channel. Its flow ranges between 83 m^3/s in April and 707 m^3/s in November (Fig. 4). The period of high flow is from October to December. Obviously, the nearshore Aph high coincided with the coastal eddies and the waters receiving the Cagayan River, while extending northwestward along the Kuroshio front (Fig. 6b).

5.1.2. Climatology

The climatological pattern of surface circulation in December, the peak of the LZS bloom, is generally similar to that observed in January 2010, but with a stronger Kuroshio intrusion penetrating into the SCS and the center of the LG shifting approximately one degree south (Fig. 7a). Both the offshore and the nearshore ADT lows found in January 2010 are present, implying that they are fundamental features of the study region in winter (Li et al., 2000, 2003). No cold center on the surface is visible corresponding to the LG (Fig. 7a), presumably due to surface heating or because upwelling is present subsurface (e.g. Shaw et al., 1996). However, a nearshore drop in temperature from the surrounding area presents in the Babuyan Channel and its vicinity (Fig. 7a). The Luzon Coastal Current appears to be the most prominent feature on the SST image, manifesting itself as the warm east wing of the LG (Fig. 7a).

Similar to that observed in January 2010, the climatological Aph high to the northwest of Luzon corresponds to the northern sector of the LG. However, the core of the Aph high separates from the center of the LG, falling in-between the Kuroshio intrusion and the LG center. The other Aph high in the vicinity of the Babuyan Channel, nevertheless, shows a center coinciding with the coastal eddy and the Cagayan River mouth (Fig. 7b).

5.1.3. Summary on the environment of the LZS bloom

In summary, the circulation pattern of the study region in the bloom season mainly consists of two systems: (1) the Kuroshio system, including its intrusion and eddy shedding in the northern LZS, as well as small cyclonic eddies and turbulence generated on the lee side of the Kuroshio in the southern LZS featured with complicated topography (capes and islands); (2) the SCS system, mainly the LG and the Luzon Coastal Current in northeastern SCS to the west of Luzon. Either in the 2010 case or in the general scenario, the offshore LZS bloom covers the northern sector of the LG, where the LG meets the Kuroshio intrusion. The nearshore LZS bloom matches not only with the Cagayan River mouth but also with island/cape mass on the lee side of the Kuroshio. The offshore and nearshore blooms have two environmental features in common: they both appear to the west of the Kuroshio front, and are more or less related to cyclonic circulations (either gyre or eddy).

5.2. Mechanisms driving the LZS bloom and the role of the Kuroshio

According to the above analysis on the bloom environment and the observation of different triggering time of the blooms as described

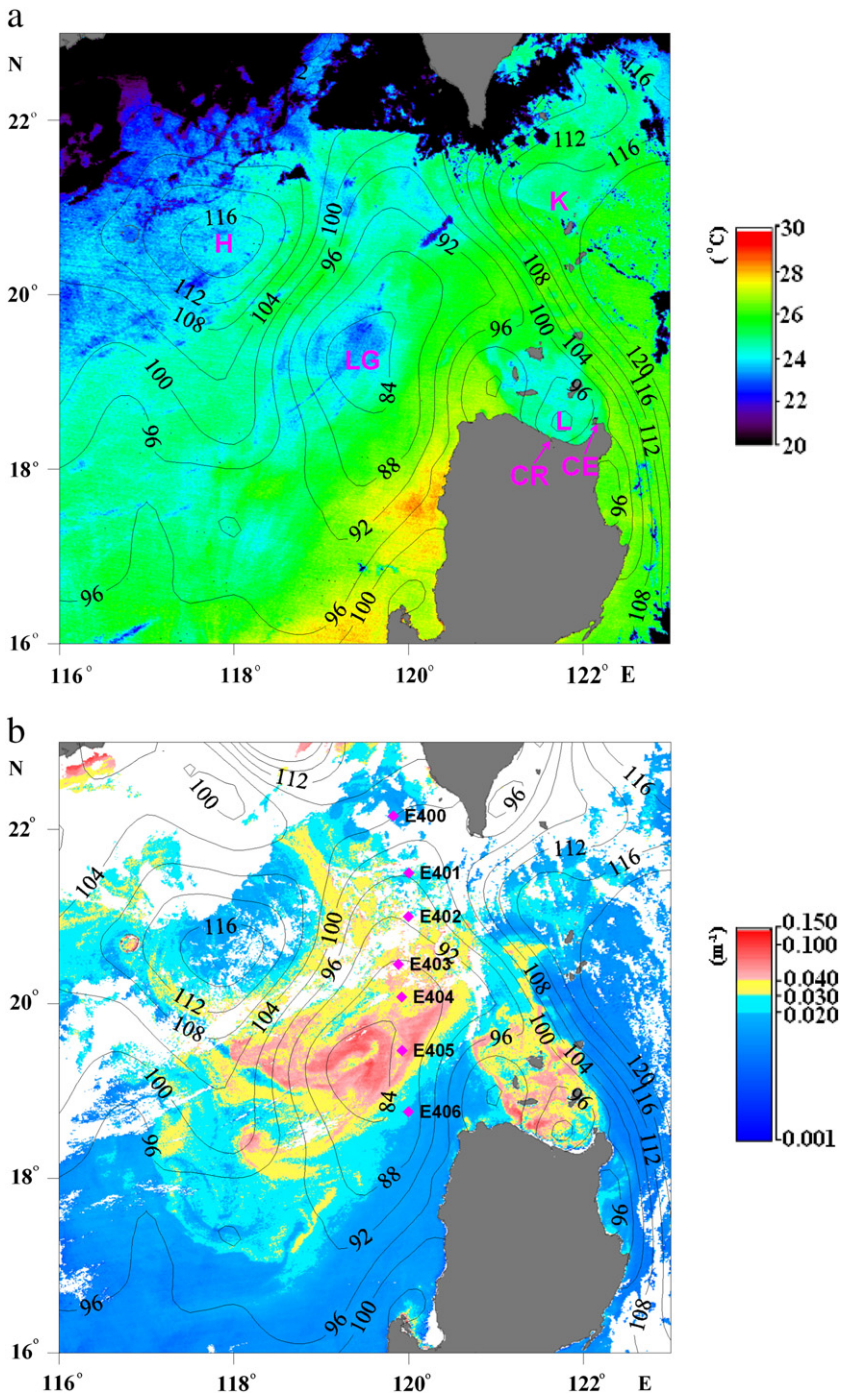

Fig. 6. (a) MODIS SST on January 28, 2010 overlaid with *Aviso* ADT (unit: cm) for January 27–February 3, 2010; the Luzon gyre (LG), ADT low (L), ADT high (H), Kuroshio (K), Cape Engano (CE) and Cagayan River (CR) are labeled; (b) MODIS Aph on January 28, 2010 overlaid with *Aviso* ADT for January 27–February 3, 2010; purple diamonds on the Aph image indicate the location of Stations E400-E406; *(c) In situ* observations of temperature (left) and salinity (right) along the E transect during January 27–30, 2010.

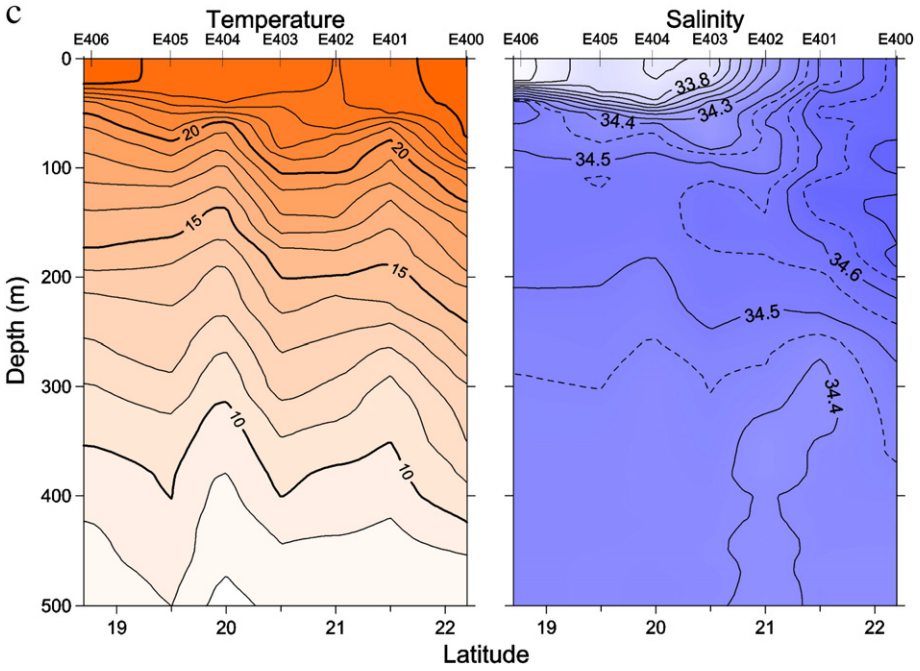

Fig. 6 (*continued*).

in Section 4, it is conceivable that there are differences in the forces underlying the nearshore and the offshore blooms.

5.2.1. Nearshore bloom

The core of the nearshore bloom agrees well with the Cagayan River mouth, either in January 2010 (Fig. 6b) or in December in general (Fig. 7b). Hence, as suggested by Penaflor et al. (2007), nutrient inputs from the northern Luzon coast, especially the Cagayan River, may facilitate this bloom and result in a band of high Aph along the northern coast of Luzon in winter. This is supported by the data in Fig. 4, which show that the blooming season mostly coincides with the flooding season of the Cagayan River. The Cagayan River discharge increases in October, when the nearshore bloom is triggered, one month ahead of the offshore bloom. Monthly mean Aph in the Babuyan channel is well correlated with the monthly mean river discharge ($R^2 = 0.51$, $n = 12$).

However, the monthly mean Aph peaks in December, when the discharge of the Cagayan River has dropped about 30%; and it maintains at a high level in January, while the river discharge has dropped to the background level (Fig. 4). Based on this temporal feature and the spatial co-incidence of the blooming patch with the cool water on the lee side of the Kuroshio, it is believed that the eddy-associated upwelling and turbulent mixing generated by the interaction of the Kuroshio with cape and island mass in the southern LZS also play an important role. Similar blooms have been widely observed in the global ocean, known as the island mass effect (e.g. Aristegui et al., 1997; Martinez & Maamaatuaiahutapu, 2004; Signorini et al., 1999).

5.2.2. Offshore bloom

In the January 2010 event, the high Aph patch of the offshore bloom was mainly located in the northern LG (Fig. 6a and b). The three centers (Aph high, ADT low, and SST low) approximating each other suggests that the bloom was induced primarily by nutrient pumping at the center of LG, where strong upwelling occurred. Meanwhile, most of the intense offshore bloom patch concentrated on the northern sector of the LG, falling in a frontal zone between the LG and the Kuroshio intrusion. This further suggests that a variety of mesoscale processes well recognized in this frontal zone may provide a mechanism under which nutrients can be brought into the euphotic zone and allow phytoplankton to thrive. These processes, generated by the interaction of the Kuroshio intrusion with the complex topography of the LZS and the LG, presumably include active eddies of different scales (e.g. Chen et al., 2007; Li et al., 1998; Metzger & Hurlburt, 2001; Wang et al., 2003), and internal waves and solitons (e.g. Liu et al., 1998; Yuan et al., 2006; Zheng et al., 2001). Cases of phytoplankton blooms associated with these processes in this frontal zone had ever been observed (e.g. Chen et al., 2007; Li & Pohlmann, 2002).

Climatologically, the high offshore Aph is also located in the northern sector of the LG, the frontal zone between the LG and the Kuroshio intrusion (Fig. 7b). However, the two centers (Aph high and ADT low) do not co-locate, and no surface cool center corresponding to the LG center is detectable (Fig. 7a), suggesting that no strong surface upwelling stably occurs at the LG center. The National Oceanographic Data Center temperature contour at 100 m depth overlaid on surface Aph lends further supports to this notion (Fig. 7c), which points to high Aph moving cyclonically around the periphery of a distinct subsurface cool center coincident with the core of the LG. Therefore, while the upwelling at the LG center may contribute to the bloom, climatologically the offshore bloom is primarily triggered and sustained by the mesoscale nutrient pumping/mixing processes in the Kuroshio intrusion-LG frontal zone, explaining why the bloom occurs most frequently in the mid-LZS bounded by 19–20°N, 120–121°E. The bloom patch triggered in the mid-LZS appears to be advecting cyclonically around the LG, losing its intensity gradually on its way to the southwest.

This discrepancy between the 2010 case and the climatological statistics implies that the physical environment nourishing the offshore bloom is very dynamic, leading to the highly variable bloom in space and time. Climatologically, the LG center is located to the west of northern Luzon (e.g. Li et al., 2003), although it may occasionally move away, as in January 2010. Most of the time the upwelling at the LG center is present subsurface, without a pool of cool water on the surface (e.g. Shaw et al., 1996). Nevertheless, the upwelling was strong in January 2010, as indicated by the MODIS SST low (Fig. 6a). These variations may possibly be due to fluctuations in the Kuroshio and the monsoonal forcing relevant to the LG. However, what exactly drives the LG shift and what changes its upwelling intensity are beyond the scope of this study.

5.2.3. Summary on the mechanisms underlying the LZS bloom

In summary, we attribute the nearshore bloom core to the Cagayan River input, as well as eddy-associated upwelling and turbulent mixing on the lee side of the Kuroshio, which are generated by the interaction of the Kuroshio with the topography of the southern LZS. And we propose that the LG upwelling is not the sole contributor to the offshore bloom core; the offshore core, very importantly, is also induced and sustained by a variety of meso-scale nutrient pumping and vertical mixing processes generated by the interaction of the Kuroshio intrusion with the LG and the complex topography of the LZS. The offshore and nearshore bloom both peak in December due to their associations with the Kuroshio and its intrusion. The Kuroshio thus plays a major role in the formation of the LZS bloom, although it does not directly supply nutrients. It leads to various processes that stir the water column, facilitating injection of nutrients from depth to the surface.

On the other hand, it can be inferred from our analysis that the LZS bloom is not a bloom per se, but a series of intermittent bloom events triggered and sustained by intermittent Kuroshio intrusions and their interaction with the LG and the LZS topography. There is no evidence that the Kuroshio intrudes into the SCS throughout the year; however, it is believed to occur during the northeast monsoon season (e.g. Li

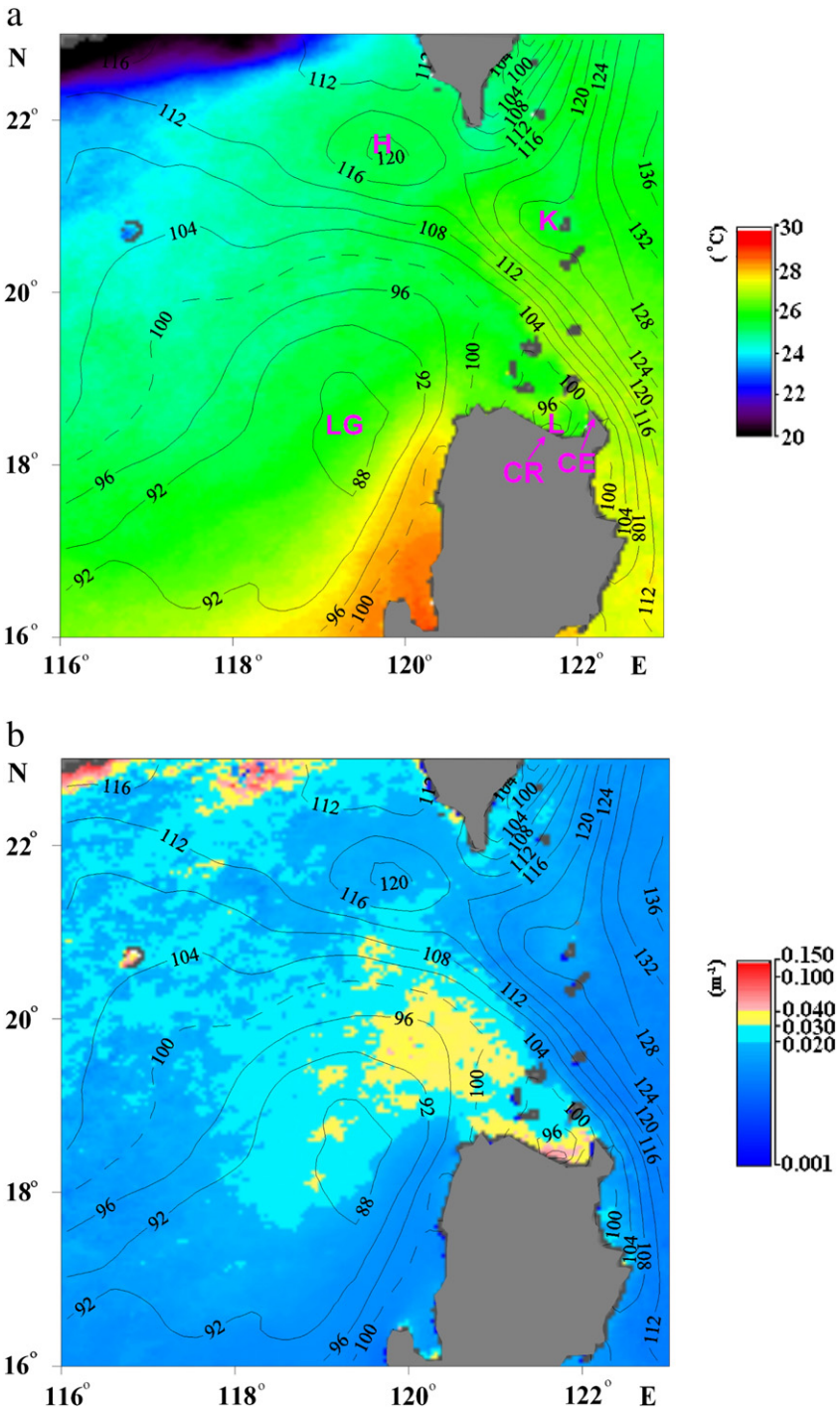

Fig. 7. (a) Climatological monthly mean MODIS SST in December overlaid with concurrent climatological monthly mean *Aviso* ADT; the Luzon gyre (LG), ADT low (L), ADT high (H), Kuroshio (K), Cape Engano (CE) and Cagayan River (CR) are labeled; (b) Climatological monthly mean MODIS Aph in December overlaid with concurrent climatological monthly mean *Aviso* ADT; (c) Climatological monthly mean MODIS Aph in December overlaid with concurrent climatological monthly mean NODT temperature at 100 m depth.

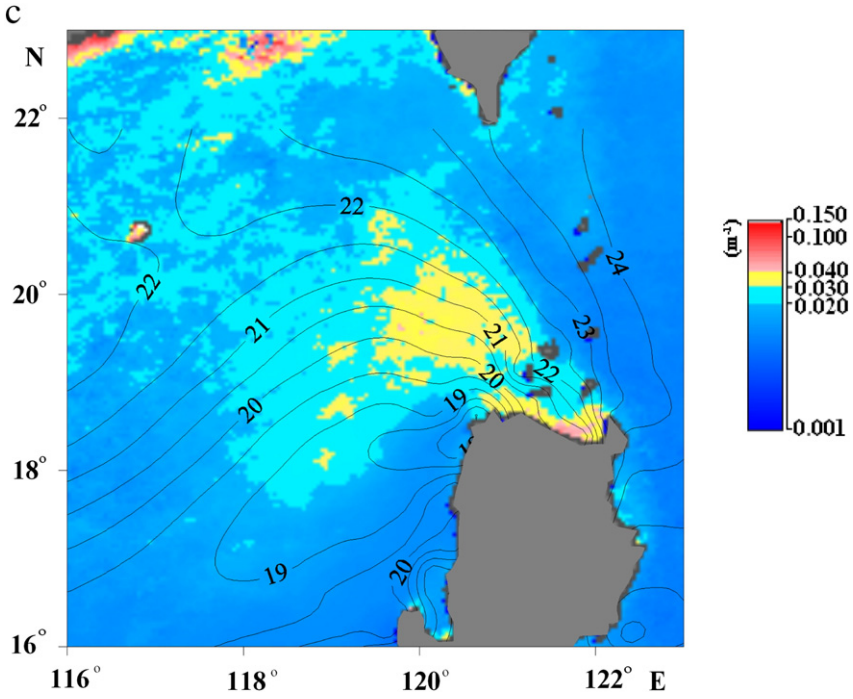

Fig. 7 (*continued*).

et al., 2003). Therefore, although the LZS bloom is only observable from November to February in the climatological case, the bloom possibly occurs beyond this period, given that the northeast monsoon is prevailing. Hence, it is unsurprising that Chen et al. (2007) captured a late-spring LZS bloom, based on *in situ* observations, SeaWiFS Chl data, and AVHRR SST data. We also processed MODIS Aph (see Fig. 8) on April 29, 2005, when Chen et al. (2007) observed the bloom event *in situ*. These data clearly show patches of high Aph ($\geq 0.02\ m^{-1}$) in the southern and mid-LZS. The mid-LZS patch centered at ~20°N, 120°E coincides with Station 5 of Chen et al. (2007), where they observed a domed thermocline, elevated nutrients, and enhanced primary production. The patch in the southern LZS, however, was not documented previously because a reliable biological index was not available in that coastal water, highlighting the advantage of including analytically-derived Aph in the interpretation of blooms.

6. Conclusions

Based on the analysis of MODIS Aph, FLH, and Chl data, together with satellite altimetry, SST, and *in situ* biological and hydrological properties, we derive the following three conclusions. First, the LZS bloom has a twin-core structure, with one core offshore in the northeast

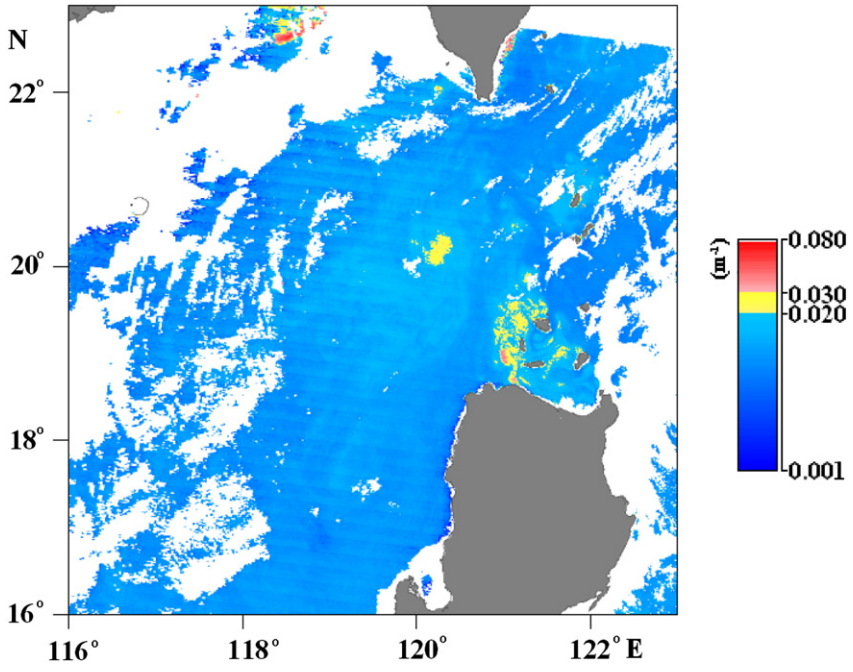

Fig. 8. MODIS Aph on April 29, 2005.

SCS basin and the other core nearshore in the Babuyan Channel. Second, climatologically the offshore bloom persists from November-February and peaks in December; the nearshore core emerges in October and peaks in December as well. Third, the offshore bloom is mainly triggered and sustained by nutrient pumping and entrainment from depth due to meso-scale processes generated by the interaction of the Kuroshio and its intrusion with the LZS topography and the sub-basin scale circulation in the northeastern SCS (i.e. the LG), while the LG upwelling contributes as well. For the nearshore bloom, nutrients are both from depth, induced by the interaction of the Kuroshio with the LZS topography, and from the Cagayan River. The Kuroshio thus plays a major role in the formation of the LZS bloom.

This study provides a fresh view of the LZS bloom both offshore and nearshore by means of a new remote sensing pigmentation index, Aph, that is derived from a quasi-analytical algorithm with the impact of colored dissolved organic matter and detritus removed. The significance of the Kuroshio and its intrusion to the formation of the LZS bloom and therefore the carbon cycling of the northeastern SCS is reinforced (Chen et al., 2007; Penaflor et al., 2007). These results provide new insights to study and understand the biogeochemistry of waters in this region. Future multi-disciplinary field campaigns in the LZS and its vicinity, especially time-series observations, are necessary to capture the high spatio-temporal variation of the bloom, and to quantify the various contributors to the formation of the bloom.

Acknowledgements

S. Shang, L. Li & J. Sun were supported by the Chinese Ministry of Science and Technology through the National Basic Research Program (#2009CB421201, #2009CB421205 and #2009CB421202). S. Shang, J. Li, Y. Li and G. Lin were also supported by the NSF-China (#40976068) and the High-Tech R & D Program (#2008AA09Z108). We thank the crew of R/V *DongFangHong II* for help collecting *in situ* data. We also thank three anonymous reviewers for their critical comments.

References

Aristegui, J., Tett, P., Hernández-Guerra, A., Basterretxea, G., Montero, M. F., Wild, K., Sangrá, P., Hernández-León, S., Canton, M., & Garcia-Braun, J. A. (1997). The influence of island-generated eddies on chlorophyll distribution: a study of mesoscale variation around Gran Canaria. *Deep Sea Research Part I: Oceanographic Research Papers*, *44*, 71–96.

Chen, L. Y. L. (2005). Spatial and seasonal variations of nitrate-based new production and primary production in the South China Sea. *Deep Sea Research Part I*, *52*, 319–340.

Chen, L. Y. L., Chen, H. Y., Lin, I. I., Lee, M. A., & Chang, J. (2007). Effects of cold eddy on phytoplankton production and assemblages in Luzon Strait bordering the South China Sea. *Journal of Oceanography*, *63*, 671–683.

Chen, C. C., Shiah, F. K., Chung, S. W., & Liu, K. K. (2006). Winter phytoplankton blooms in the shallow mixed layer of the South China Sea enhanced by upwelling. *Journal of Marine Systems*, *59*, 97–110.

Cullen, J. J. (1982). The deep chlorophyll maximum: comparing vertical profiles of chlorophyll a. *Canadian Journal of Fisheries and Aquatic Sciences*, *39*, 791–803.

Dong, Q., Hong, H., & Shang, S. (2008). A new approach to correct for pathlength amplification in measurements of particulate spectral absorption by the quantitative filter technique. *Journal of Xiamen University (Natural Science)*, *47*, 556–561 (in Chinese with an English abstract).

Fang, G., Fang, W., Fang, Y., & Wang, K. (1998). A survey of studies on the South China Sea upper ocean circulation. *Acta Oceanographica Taiwanica*, *37*, 1–16.

Gower, J. (1980). Observations of in situ fluorescence of chlorophyll-a in Saanich Inlet. *Boundary-Layer Meteorology*, *18*, 235–245.

Hirawake, T., Takao, S., Horimoto, N., Ishimaru, T., Yamaguchi, Y., & Fukuchi, M. (2011). A phytoplankton absorption-based primary productivity model for remote sensing in the Southern Ocean. *Polar Biology*, *34*, 291–302.

Hu, C. M., Chen, Z. Q., Clayton, T. D., Swarzenski, P., Brock, J. C., & Muller-Karger, F. E. (2004). Assessment of estuarine water-quality indicators using MODIS medium-resolution bands: Initial results from Tampa Bay, FL. *Remote Sensing of Environment*, *93*, 423–441. http://dx.doi.org/10.1016/j.rse.2004.08.007.

Hu, J., Zheng, Q., Sun, Z., & Tai, C. K. (2012). Penetration of nonlinear Rossby eddies into South China Sea evidenced by cruise data. *Journal of Geophysical Research*, *117*, C03010.

Kiefer, D. A., & SooHoo, J. B. (1982). Spectral absorption by marine particles of coastal waters of Baja California. *Limnology and Oceanography*, *27*, 492–499.

Kishino, M., Takahashi, M., Okami, N., & Ichimura, S. (1985). Estimation of the spectral absorption coefficients of phytoplankton in the sea. *Bulletin of Marine Science*, *37*, 634–642.

Lee, Z. P., Arnone, R., Hu, C. M., Werdell, P. J., & Lubac, B. (2010). Uncertainties of optical parameters and their propagations in an analytical ocean color inversion algorithm. *Applied Optics*, *49*, 369–381.

Lee, Z. P., Carder, K. L., & Arnone, R. A. (2002). Deriving inherent optical properties from water color: a multiband quasi-analytical algorithm for optically deep waters. *Applied Optics*, *41*, 5755–5772.

Lee, Z. P., Carder, K. L., Marra, J., Steward, R. G., & Perry, M. J. (1996). Estimating primary production at depth from remote sensing. *Applied Optics*, *35*(2), 463–474.

Lee, Z., Lance, V. P., Shang, S., Vaillancourt, R., Freeman, S., Lubac, B., Hargreaves, B. R., Del Castillo, C., Miller, R., & Twardowski, M. (2011). An assessment of optical properties and primary production derived from remote sensing in the Southern Ocean (SO GasEx). *Journal of Geophysical Research*, *116*, C00F03. http://dx.doi.org/10.1029/2010JC006747.

Lee, Z. P., Weidemann, A., Kindle, J., Amone, R., Carder, K. L., & Davis, C. (2007). Euphotic zone depth: Its derivation and implication to ocean-color remote sensing. *DTIC Document*.

Letelier, R. M., & Abbott, M. R. (1996). An analysis of chlorophyll fluorescence algorithms for the moderate resolution imaging spectrometer (MODIS). *Remote Sensing of Environment*, *58*, 215–223.

Li, L., Nowlin, W., & Su, J. (1998). Anticyclonic rings from the Kuroshio in the South China Sea. *Deep Sea Research Part I: Oceanographic Research Papers*, *45*, 1469–1482.

Li, L., & Pohlmann, T. (2002). The South China Sea warm-core ring 94S and its influence on the distribution of chemical tracers. *Ocean Dynamics*, *52*, 116–122.

Li, L., Wu, R., & Guo, X. (2000). Seasonal circulation in the South China Sea — a TOPEX/POSEIDON satellite altimetry study. *Acta Oceanologica Sinica*, *22*.

Li, L., Xu, J., Jing, C., Wu, R., & Guo, X. (2003). Annual variation of sea surface height, dynamic topography and circulation in the South China Sea. *Science in China Series D: Earth Sciences*, *46*, 127–138.

Liu, A. K., Chang, Y. S., Hsu, M. K., & Liang, N. K. (1998). Evolution of nonlinear internal waves in the East and South China Seas. *Journal of Geophysical Research*, *103*, 7995–8008.

Liu, K. K., Chao, S. Y., Shaw, P. T., Gong, G. C., Chen, C. C., & Tang, T. (2002). Monsoon-forced chlorophyll distribution and primary production in the South China Sea: observations and a numerical study. *Deep Sea Research Part I*, *49*, 1387–1412.

Locarnini, R. A., Mishonov, A., Antonov, J., Boyer, T., & Garcia, H. (2006). World Ocean Atlas 2005. *Temperature*, *1*.

Marra, J., Trees, C. C., & O'Reilly, J. E. (2007). Phytoplankton pigment absorption: a strong predictor of primary productivity in the surface ocean. *Deep Sea Research Part I*, *54*, 155–163.

Martinez, E., & Maamaatuaiahutapu, K. (2004). Island mass effect in the Marquesas Islands: Time variation. *Geophysical Research Letters*, *31*, L18307.

Metzger, E. J., & Hurlburt, H. E. (2001). The nondeterministic nature of Kuroshio penetration and Eddy shedding in the South China Sea*. *Journal of Physical Oceanography*, *31*, 1712–1732.

O'Reilly, J. E., Maritorena, S., Siegel, D. A., O'Brien, M. C., Toole, D., Mitchell, B. G., Kahru, M., Chavez, F. P., Strutton, P., & Cota, G. F. (2000). Ocean color chlorophyll a algorithms for SeaWiFS, OC2, and OC4: Version 4. *SeaWiFS postlaunch calibration and validation analyses, Part, 3* (pp. 9–23).

Penaflor, E. L., Villanoy, C. L., Liu, C. T., & David, L. T. (2007). Detection of monsoonal phytoplankton blooms in Luzon Strait with MODIS data. *Remote Sensing of Environment*, *109*, 443–450.

Shang, S., Dong, Q., Lee, Z., Li, Y., Xie, Y., & Behrenfeld, M. (2011). MODIS observed phytoplankton dynamics in the Taiwan Strait: an absorption-based analysis. *Biogeosciences*, *8*, 841–850.

Shaw, P. T., & Chao, S. Y. (1994). Surface circulation in the South China Sea. *Deep Sea Research Part I: Oceanographic Research Papers*, *41*, 1663–1683.

Shaw, P. T., Chao, S. Y., Liu, K. K., Pai, S. C., & Liu, C. T. (1996). Winter upwelling off Luzon in the northeastern South China Sea. *Journal of Geophysical Research*, *101*, 16435–16448.

Signorini, S. R., McClain, C. R., & Dandonneau, Y. (1999). Mixing and phytoplankton bloom in the wake of the Marquesas Islands. *Geophysical Gesearch letters*, *26*, 3121–3124.

Tang, D. L., Ni, I. H., Kester, D. R., & Muller-Karger, F. E. (1999). Remote sensing observations of winter phytoplankton blooms southwest of the Luzon Strait in the South China Sea. *Marine Ecology Progress Series*, *191*, 43–51.

Tassan, S., & Ferrari, G. M. (2002). A sensitivity analysis of the 'Transmittance-Reflectance' method for measuring light absorption by aquatic particles. *Journal of Plankton Research*, *24*, 757–774.

Udarbe-Walker, M. J. B., & Villanoy, C. L. (2001). Structure of potential upwelling areas in the Philippines. *Deep Sea Research Part I*, *48*, 1499–1518.

Wang, G., Su, J., & Chu, P. C. (2003). Mesoscale eddies in the South China Sea observed with altimeter data. *Geophysical Research Letters*, *30*, 2121.

Wang, J. J., Tang, D. L., & Sui, Y. (2010). Winter phytoplankton bloom induced by subsurface upwelling and mixed layer entrainment southwest of Luzon Strait. *Journal of Marine Systems*, *83*, 141–149.

Wang, D., Xu, H., Lin, J., & Hu, J. (2008). Anticyclonic eddies in the northeastern South China Sea during winter 2003/2004. *Journal of Oceanography*, *64*, 925–935.

Wyrtki, K. (1961). Scientific results of marine investigations of the South China Sea and the Gulf of Thailand 1959–1961. *NAGA report*, *2*.

Yuan, Y., Zheng, Q., Dai, D., Hu, X., Qiao, F., & Meng, J. (2006). Mechanism of internal waves in the Luzon Strait. *Journal of Geophysical Research*, *111*.

Zheng, Q., Klemas, V., Yan, X. H., & Pan, J. (2001). Nonlinear evolution of ocean internal solitons propagating along an inhomogeneous thermocline. *Journal of Geophysical Research*, *106* (14083–14014,14094).